

Effects of Variable Normal Stress on Rock Friction: Observations and Constitutive Equations

M. F. LINKER¹ AND J. H. DIETERICH

U.S. Geological Survey, Menlo Park, California

We investigate the effects of variable normal stress on frictional resistance by performing quasi-static sliding experiments with 5×5 cm blocks of Westerly granite in a double-direct shear apparatus under servo-control. The observed response to a change in normal stress mimics that which occurs in response to a change in slip velocity. In particular, a sudden change in normal stress results in a sudden change followed by a transient change in the resistance to sliding. We interpret these changes within the previously established constitutive framework in which frictional resistance is determined by the current slip speed V , the current normal stress, and the state of the sliding surface (Dieterich, 1979a, 1981; Ruina, 1980, 1983). Earlier work demonstrated that the state of the sliding surface depends on prior slip speed. Our observations indicate that the state of the sliding surface also depends on prior normal stress. In our model the functional dependence of state on normal stress is expressed in terms of the same state variable, θ , used previously to represent slip rate history effects. We assume that the steady state value of θ is independent of normal stress and that $\theta^{ss} = D_c/V$, where D_c is a characteristic slip distance. We interpret the variable θ as a measure of effective contact time. At constant slip speed and from an initial steady state, a sudden change in normal stress results in a sudden change in θ followed by a gradual change in θ back toward the initial θ^{ss} , as sliding proceeds. The magnitude of the sudden change in θ is determined by a newly identified parameter that we call α . Earlier workers have established that stability is influenced by stiffness, $d\tau^{ss}/dV$, D_c , and slip rate history (Rice and Ruina, 1983). We conclude that stability will also be influenced by normal stress history and by α .

1. INTRODUCTION

Friction laws incorporating slip rate and surface state dependence have been proposed [Dieterich, 1979a, 1981; Ruina, 1983] to simulate the observed frictional behavior of rock in laboratory experiments [Dieterich, 1979a, 1981; Ruina, 1980, 1983; Okubo and Dieterich, 1984, 1986; Weeks and Tullis, 1985; Tullis and Weeks, 1986; Chester, 1988; Biegel et al., 1989; Marone et al., 1990; Wong et al., 1991; Blanpied et al., in press]. The utility of these laws is demonstrated by their incorporation in numerous attempts to simulate fault slip in the Earth. These studies include stability analyses [Ruina, 1980; Rice and Ruina, 1983; Gu et al., 1984; Blanpied and Tullis, 1986; Horowitz, 1988], the quasi-static nucleation and growth of unstable fault slip [Dieterich, 1979b, 1986], the analysis of dynamic motion [Okubo and Dieterich, 1986; Rice and Tse, 1986; Okubo, 1989], the triggering of large crustal earthquakes and aftershocks [Rice and Gu, 1983; Dieterich, 1987, 1988], the modeling of creep events [Marone et al., 1991], and finally, efforts to simulate the entire cycle of crustal earthquakes [Tse and Rice, 1986; Stuart, 1988; Horowitz and Ruina, 1989; G. M. Mavko, unpublished manuscript, 1984].

For a fault to exhibit unstable slip, i.e., seismicity, the sliding resistance must decrease with displacement. Perhaps the simplest representation of this behavior is the slip-weakening model. Furthermore, for a fault to exhibit repeated unstable slip, some healing process must also take place. The rate- and state-dependent friction laws not only

yield slip weakening, whenever the stress is greater than some reference value, but also result in time-dependent healing of the fault, whenever the shear stress is less than that reference value. The stress at the transition from healing to weakening corresponds to steady state sliding.

To date, the major focus in the laboratory has been to describe the variation in the resistance to sliding under conditions of variable slip rate at constant normal stress. Under these conditions, according to the rate- and state-dependent model, the resistance to sliding can be specified if the current slip speed and prior slip speed history are known. However, both in the Earth and in laboratory experiments, the assumption of constant normal stress is often not appropriate.

Only under very unusual and idealized situations does a change in the applied stress, resolved onto a sliding surface, simplify to a change in shear traction alone. For example, Mavko et al. [1985] observed that the May 1983 Coalinga, California, earthquake had an immediate effect on creep rates along the San Andreas fault and calculated that the static coseismic change in normal stress resolved onto the San Andreas fault exceeded the change in shear stress by at least a factor of 2. Another familiar example is the conventional triaxial test where the axial load and the confining pressure together contribute to both the normal stress and the shear stress on the sliding surface so that changes in axial load necessarily lead to changes in normal stress, unless the confining pressure is continuously and very precisely compensated. This task of compensation is very difficult, if not impossible during rapid slip.

Preliminary investigations on the transient effects of changes in normal stress on the resistance to sliding have been performed by Hobbs and Brady [1985], Lockner et al. [1986], and Olsson [1988]. All workers made similar observations; in response to a sudden increase in normal stress the

¹Now at Department of Earth and Planetary Sciences, Harvard University, Cambridge, Massachusetts.

This paper is not subject to U.S. copyright. Published in 1992 by the American Geophysical Union.

Paper number 92JB00017.

resistance to sliding rises suddenly and then continues to rise toward a new steady state value as sliding proceeds. A step decrease in normal stress appears to yield similar results, with a sudden decrease in shear stress followed by a displacement dependent decay toward the new steady state value. Interpretation of these latter data is made more difficult by the tendency for instability.

In this paper we investigate and characterize the transient variation in the resistance to sliding that results from changes in normal stress. We present data demonstrating that a sudden change in normal stress produces both a sudden and a transient variation in the resistance to sliding, similar in form to those observed in response to an imposed velocity step and consistent with observations made in the previous studies noted above.

2. THEORETICAL FRAMEWORK

In this section we present a brief review of the previously established framework, developed to describe the effects of variable slip rate, and describe how the effects of variable normal stress can be incorporated.

Observations from earlier experiments can be summarized as follows. At constant normal stress σ and fixed load point velocity, the resistance to sliding, τ , evolves toward a steady state value that depends on the slip velocity V . In response to an imposed step increase in load point velocity, the resistance to sliding increases suddenly but then decays toward a new steady state value as sliding proceeds. The decay roughly follows an exponential with characteristic displacement D_c , and the new steady state shear stress depends on the new slip velocity. The response to a step decrease in load point velocity is fairly symmetric to that observed in response to a velocity increase. In some experiments the decay to steady state in response to a jump in load point velocity may better be described by two decay constants [Ruina, 1980, 1983; Weeks and Tullis, 1985; Tullis and Weeks, 1986].

Dieterich [1979a] argued that under the conditions of constant normal stress, the resistance to sliding can be described by the current slip velocity and a parameter θ that represents the effective age of contacting asperities on the sliding surface and which in turn depends on the slip velocity history. Following an imposed step change in slip velocity, the effective age of the contacts gradually becomes proportional to the inverse of the new slip velocity as sliding proceeds. That is, θ evolves continuously to a steady state value proportional to $1/V$. This interpretation of θ as the effective age of contacts was originally motivated by the observation of the linear increase in "static" friction with the logarithm of the duration of contact [Dieterich, 1972] and the common observation, from indentation tests, that the area of contact under the indenter also increases linearly with the logarithm of the contact time [Scholz and Engelder, 1976]. Dieterich and Conrad [1984] later demonstrated that the so-called θ effects disappear under ultradry conditions, just as the indentation-creep effect disappears during tests with ultradry surfaces.

Ruina [1983] and more explicitly Rice and Ruina [1983] noted that the state of the sliding surface could depend not only on prior slip rate but also on prior normal stress. Following their work, we write

$$\tau(t) = F[V(t), \sigma(t), \theta_1(t), \theta_2(t), \theta_3(t), \dots, \theta_n(t)] \quad (1)$$

$$d\theta_i/dt = G_i[V(t), \sigma(t), \theta_1(t), \theta_2(t), \theta_3(t), \dots, \theta_n(t)]. \quad (2)$$

Here we have admitted that more than one state variable may be necessary to characterize changes in τ and that the evolution laws governing the variation in the state variables may be functions of slip velocity, normal stress, and the state variables themselves, θ_i .

In this paper we employ a version of Ruina's [1980, 1983] simplification of the friction law proposed by Dieterich [1979a, 1981]:

$$\tau = \mu^* \sigma + A \sigma \ln(V/V^*) + B \sigma \ln(\theta/\theta^*), \quad (3)$$

where μ^* represents a constant reference value of the coefficient of friction and θ is a scalar variable that represents the state of the sliding surface. If we assume that the steady state value of θ^* is independent of normal stress, then when $V = V^*$ at steady state, $\theta = \theta^*$ and $\tau = \mu^* \sigma$. In (3) the coefficients A and B are constitutive parameters that we estimate from laboratory measurements, and the variation of θ is governed by an evolution law that, in general, may include normal stress dependence.

Two evolution laws have been proposed to describe the variation in θ with slip, δ , at fixed normal stress:

$$\left(\frac{\partial \theta}{\partial \delta}\right)_{\sigma = \text{const}} = \frac{1}{V} - \frac{\theta}{D_c} \quad (4)$$

and

$$\left(\frac{\partial \theta}{\partial \delta}\right)_{\sigma = \text{const}} = \left(\frac{-\theta}{D_c}\right) \ln\left(\frac{\theta V}{D_c}\right). \quad (5)$$

At steady state, $d\theta/dt = 0$, and both (4) and (5) yield $\theta^{ss} = D_c/V$. The solution of these evolution laws under the condition of constant slip speed are

$$\theta = \frac{D_c}{V} + \left(\theta_0 - \frac{D_c}{V}\right) \exp\left(\frac{\delta_0 - \delta}{D_c}\right) \quad (6)$$

and

$$\theta = \left(\frac{D_c}{V}\right) \left(\frac{\theta_0 V}{D_c}\right)^{\exp[(\delta_0 - \delta)/D_c]} \quad (7)$$

for equations (4) and (5), respectively, where $\theta = \theta_0$ when $\delta = \delta_0$. Equation (4) was originally proposed by Ruina [1980, 1983] but later used extensively by Dieterich [1981, 1986, 1987]. Equation (7) was initially proposed by Dieterich [1979a] and then presented in differential form (5) by Kosloff and Liu [1980] and Ruina [1980, 1983]. Ruina [1983] and several other workers (see, for example, Koslov and Liu [1980], Gu et al. [1984], Rice and Tse [1986], Tullis and Weeks [1986], and Stuart [1988]) have employed similar formulations corresponding to equations (3) through (7), but using an alternate representation for the state variable. In Appendix A we outline the algebraic equivalence of equations (3) through (7) to those used by Ruina [1983] and later by others. There we also present our proposed formulation

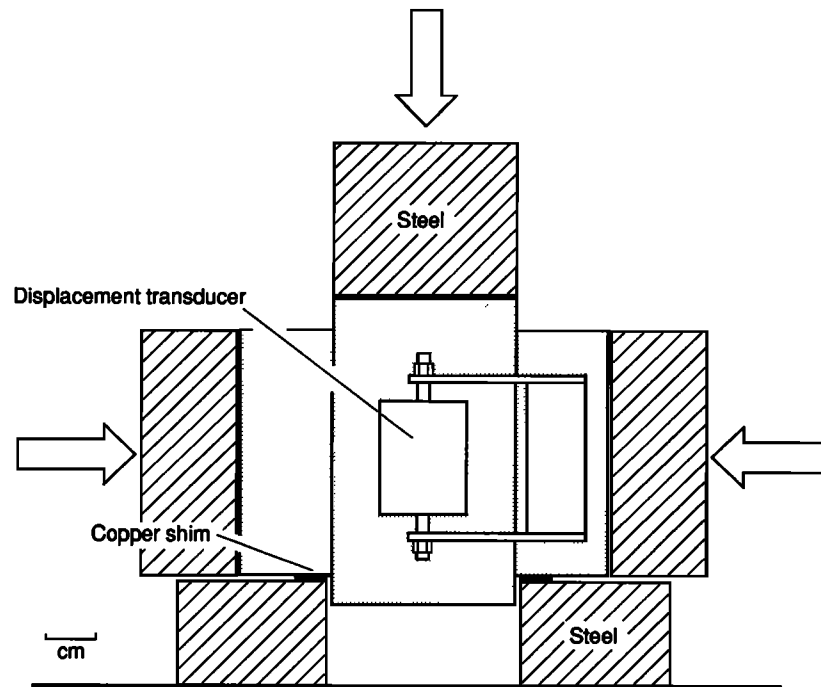


Fig. 1. Sample assembly and configuration of applied loads for the double direct shear apparatus. The displacement transducer is mounted directly on the specimen.

for normal stress dependence, as developed later in this paper, but using the alternative definition of state.

We next present our experimental observations and then extend the previously proposed evolution laws, equations (4) and (5), to incorporate the effects of variable normal stress on state. In Appendix B we offer a physical interpretation of state that considers changes in normal stress and is consistent with both classical friction theory and earlier interpretations of θ .

3. EXPERIMENTAL PROCEDURE

All of the tests were performed in the double direct shear apparatus employed by *Dieterich* [1972, 1981] and *Ruina* [1983]. We have modified the apparatus to allow for rapid servo-control of both normal stress and load point displacement. We aligned and tested the two nominally perpendicular loading frames in an effort to maximize the degree to which the two independently controlled hydraulic rams individually provide the applied normal stress and shear stress. In addition, we mounted the displacement transducer (DCDT) directly on the sample (Figure 1) to minimize interactions between normal stress control and load point displacement and to increase the load point stiffness. The resulting load point stiffness is about $0.5 \text{ MPa}/\mu\text{m}$. Even with our improvements to the apparatus, imposed changes in horizontal load do result in small, measurable changes in vertical load. That is, imposed changes in normal stress result in small changes in shear stress. These changes in shear stress are fully recoverable, and their magnitude appears to scale linearly with the magnitude of imposed change in normal stress. The measured coupling coefficient, $S \equiv \Delta\tau/\Delta\sigma$, is about 0.2. We conclude that the source of the coupling is purely elastic and is probably caused by Poisson's effect within the sample and slight misalignment of the apparatus, which together result in an error signal that is sent

to the displacement servo and which in turn results in a change in vertical load that accompanies an imposed change in horizontal load. Later, using numerical simulations, we will show how this elastic coupling complicates the data analysis but does not affect our major conclusions.

For the purposes of this paper, we employ the manufacturer-supplied transducer sensitivity for determining displacement and expect that these values are accurate to about 10% or better. We have amplified the output of the DCDT so that a change of 1 mV corresponds to a displacement of the load point of about $0.02 \mu\text{m}$.

We selected commercial load cells that allow measurement of changes in shear and normal stress precise to about 0.009 and 0.004 MPa, respectively. At a normal stress of 5.0 MPa this precision corresponds to better than 0.1% for normal stress changes. After performing these tests, we discovered a calibration error that leads to systematic errors of about 5% in normal stress and in the coefficient of friction. To avoid the awkward numerical values that result from the corrections of this error, the values of normal stress reported here are the nominal values that do not take this calibration error into account. To obtain the actual values, one should multiply the values reported here by 0.95. Servo-control of normal stress approaches the resolution of the amplified load cell output and corresponds to about 0.01 MPa, or about 0.2% at 5.0 MPa. The loop gain for control of normal stress is adjusted to minimize overshoot in response to commanded step changes, while still maintaining reasonably rapid response. A commanded step in normal stress of 2.5 MPa requires less than 150 ms, and the overshoot is about 0.01 MPa. The response time for displacement servo-control through the vertical ram is similarly rapid. Shear stress, normal stress, and load point displacement were recorded as analog records using low-speed strip chart and xy recorders. The amplified output of the normal stress load cell was

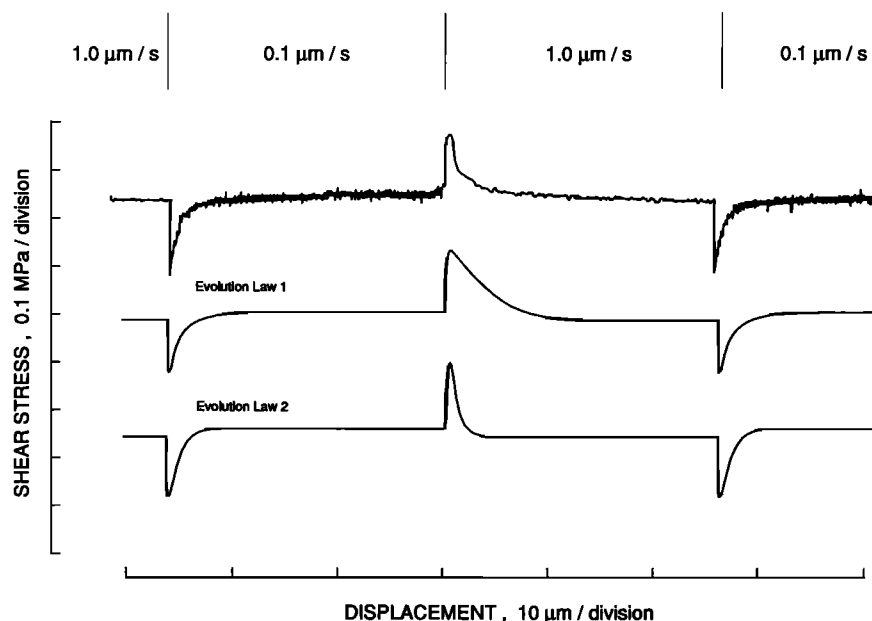


Fig. 2. Shear stress on the sliding surface versus load point displacement for representative tests in which the load point velocity is stepped by one decade. The normal stress is held constant at 5 MPa. The top curve is data. The lower two curves are simulations, which include the effects of load point stiffness and are based on equation (3) and the two evolution laws 1 and 2 represented by equations (4) and (5), respectively. The parameter values used in the simulations are listed in Table 1. The load point stiffness is sufficiently high, as indicated by the nearly vertical rise in shear stress in response to a step increase in load point displacement rate, so that the abscissa can be considered to represent displacement on the sliding surface.

additionally monitored with a digital voltmeter and an oscilloscope.

The sliding tests were performed on blocks of Westerly granite with 5×5 cm sliding surfaces. All of the friction tests were performed with surfaces that were initially ground flat on a surface grinder and then lapped by hand using #60 grit silicon carbide and water on a glass plate. The extent of the lapping guaranteed that the relic surface was completely removed. Following lapping, the sliding surface was within 0.025 mm of flat and parallel to the reference surface. Surface profiles of representative samples were measured with a profilometer carrying a 40- μ m-radius tip [Okubo, 1986]. Prior to the friction tests the rms roughness of the samples was about 19 μ m.

Newly lapped samples were preconditioned by sliding them for several millimeters at a velocity of 10 μ m/s and a normal stress of 5.0 MPa until shear stress stabilized to within about 0.01 MPa during displacement of 100 μ m. This preconditioning typically involved 6 mm of displacement. The data reported below disregard long-term drift, which is always within the 0.01 MPa per 100 μ m limit.

Following the tests, we inspected the sliding surfaces under a hand lens and observed that the wear pattern is surprisingly uniform across the sample. The sliding surfaces become covered with a light dusting of rock flour as a result of the sliding test.

4. OBSERVATIONS

The Experiments

We performed four types of frictional sliding tests. In the first type, step changes in load point velocity are imposed and the normal stress is held constant for the duration of the

test. This is the standard velocity stepping test that has been performed by earlier workers. In the three remaining tests, referred to as normal stress step, normal stress pulse, and hold-pulse tests, the normal stress is altered during the test. In all tests the reference normal stress was 5.0 MPa, and the nominal load point speed was 1 μ m/s. All tests were performed from an initial steady state shear stress.

In this section we present observations from only the velocity step, normal stress step, and normal stress pulse tests. The fourth test, the hold-pulse test, is presented and discussed later in section 6 ("tests of the proposed constitutive law"), since its interpretation is substantially more involved than that of the other three tests and since its main purpose is to test our model, rather than to help develop or constrain it.

Velocity Stepping Tests

Velocity stepping tests, analogous to those of Dieterich [1979a, 1981], Ruina [1983], Weeks and Tullis [1985], and Tullis and Weeks [1986], were performed to estimate the value of constitutive parameters related to changes in imposed slip rate at constant normal stress, i.e., A , B , and D_c . These constitutive parameters are later included in our analysis of the effects of variable normal stress. The slip rates ranged from 0.05 to 2.0 μ m/s, and the imposed changes in slip rate were one decade. Our observations are consistent with the references cited above. As these earlier workers have observed, in response to a step increase in load point velocity, the shear stress rapidly increases and then decays to a new, steady value as sliding proceeds (Figure 2). The decay to steady state shear stress roughly follows an exponential with a characteristic displacement, D_c , of about 1 to

TABLE 1. Model Parameters Determined Directly From the Experimental Records (Data) and Numerical Simulations Using Evolution Law 1 and Evolution Law 2

	Data	Law 1*	Law 2*
<i>A</i>	0.0104 ± 0.0007†	0.012	0.0145
<i>B</i>	0.0116 ± 0.0008†	0.0135	0.016
<i>D_c</i>	1–2 μm‡	2.25 μm	1.0 μm
<i>α</i>	0.20§	0.23	0.56
<i>S</i>	0.18 ± 0.03¶		
<i>K</i>	0.5 ± 0.1 MPa/μm¶		

*Values listed below were determined by trial and error, in numerical simulations of the experiments, to simultaneously best represent the experimental records from all of the tests.

†Least squares fit, and accompanying standard deviation, to data from 11 velocity steps.

‡Estimated by fitting an exponential to two points of the decay curves from the velocity stepping tests. The range represents the variation among the experiments, not the error due to the estimation method.

§Least squares fit to the data in Figure 5.

¶The uncertainty represents the variation among the data, but not in a rigorous statistical sense.

2 μm. The response to a step decrease in load point velocity is approximately symmetric to that of a step increase. That is, a rapid decrease of shear stress is followed by an asymptotic rise toward a new steady state value as sliding proceeds. In all of our velocity stepping tests, the steady state shear stress decreases very slightly with increasing slip velocity. This behavior is commonly referred to as steady state velocity weakening.

Our estimates of the parameters *A*, *B*, (equation (3)), and *D_c*, based on the velocity stepping tests, are listed in Table 1. The values listed in the data column represent mean and standard deviations from 11 step increases and decreases in load point velocity. For each step change in load point velocity, *A*, *B*, and *D_c* were determined directly from the experimental records under the assumption that a step change in load point velocity results in a equivalent step change in slip rate, or rather, that the load point stiffness is infinite. We further assumed that in response to an instantaneous step increase in slip velocity, *θ* remains constant so that the resulting jump in friction is a measure of *A*. With continued sliding at the new slip speed, *θ* evolves toward a new steady state value that depends on the new slip velocity so that the magnitude of the decay in shear stress is a measure of *B*. We estimated values of *D_c* by assuming that the decay of *τ* follows an exponential (substitute (7) into (3)). In our fitting procedure, only two points on each decay curve were used to determine *D_c*. We estimate that the uncertainty in this measurement of *D_c*, due to the variation in the data, is about a factor of 2.

Normal Stress Step Tests

Normal stress step tests consist of a step change in normal stress during sliding at fixed load point velocity of 1 μm/s. Both steps up from and steps down to the nominal 5.0-MPa normal stress were imposed. Similar tests were performed by *Hobbs and Brady* [1985], *Lockner et al.* [1986], and *Olsson* [1988].

Following a step in normal stress, sliding was continued until the shear stress versus displacement record appeared flat. At this point, another step was introduced. The entire

process was repeated until the DCDT reached its displacement limit. Step changes in normal stress of 1, 2, 4, 5, 10, 20, and 40% of 5.0 MPa were imposed. Several tests were performed for each amplitude.

Figure 3 shows representative shear stress versus load point displacement records from the normal stress step tests. As indicated in the figure, a step increase in normal stress causes a sudden increase in shear stress, due to the elastic coupling between normal stress and shear stress, by an amount indicated by the diamonds. As displacement of the load point continues, the shear stress rises further, now along the elastic loading curve of the load point. Eventually, the shear stress versus displacement path departs from the elastic loading curve, at a point indicated by the dots in Figure 3, and increases asymptotically toward a new value that is independent of displacement. The asymptotic rise toward steady state roughly follows an exponential. Interestingly, the characteristic displacement associated with the normal stress steps is about the same magnitude as that observed in the velocity step tests. To see this, compare the decay curves of Figure 3 with those of Figure 2.

The response to a step decrease in normal stress is roughly symmetric to that of a step increase. However, owing to the finite stiffness of the load point and the finite response time of the displacement servo, sudden drops in normal stress tend to result in less well controlled slip. Because of this complication, we have chosen not to include the data from downward steps in our analysis. Not surprisingly, very large step decreases in normal stress lead to unstable sliding.

The amplitude of both the total change in *τ* and the displacement-dependent change in *τ* increase with the amplitude of the normal stress step. Likewise, the duration of loading along the elastic loading curve increases with the amplitude of the normal stress step and is generally less than 1 s. The steady state coefficient of friction, about 0.7, is approximately unaffected by the change in normal stress.

The distinction between the elastic coupling of shear stress to normal stress versus loading along the elastic loading curve of the load point is not obvious in reproductions of the shear stress versus displacement records (Figure 3), and we have no high-speed recordings with which to easily demonstrate the temporal details during this early portion of the test. However, while we were performing the experiments, the distinction between the two processes was quite obvious. The former occurred immediately upon the increase in normal stress, while the latter occurred relatively slowly.

The transient effects that we have observed are in general agreement with those made by *Hobbs and Brady* [1985] and by *Olsson* [1988]. However, in the normal stress step tests by *Hobbs and Brady*, audible seismic events accompanied not only decreases but also increases in normal stress. *Olsson* occasionally observed slight overshoot of the shear stress in response to increases in normal stress. We expect that both of these effects are due to the interaction of the testing machine with the specimen rather than being intrinsically related to the constitutive behavior of the rock. *Lockner et al.* [1986] similarly concluded that all of the transient effects observed in their experiments were a result of variations in slip rate owing to the interaction of the load point stiffness and the frictional behavior of the rock.

In the normal stress step tests, during the period while shear stress rises along the elastic loading curve, the slip rate

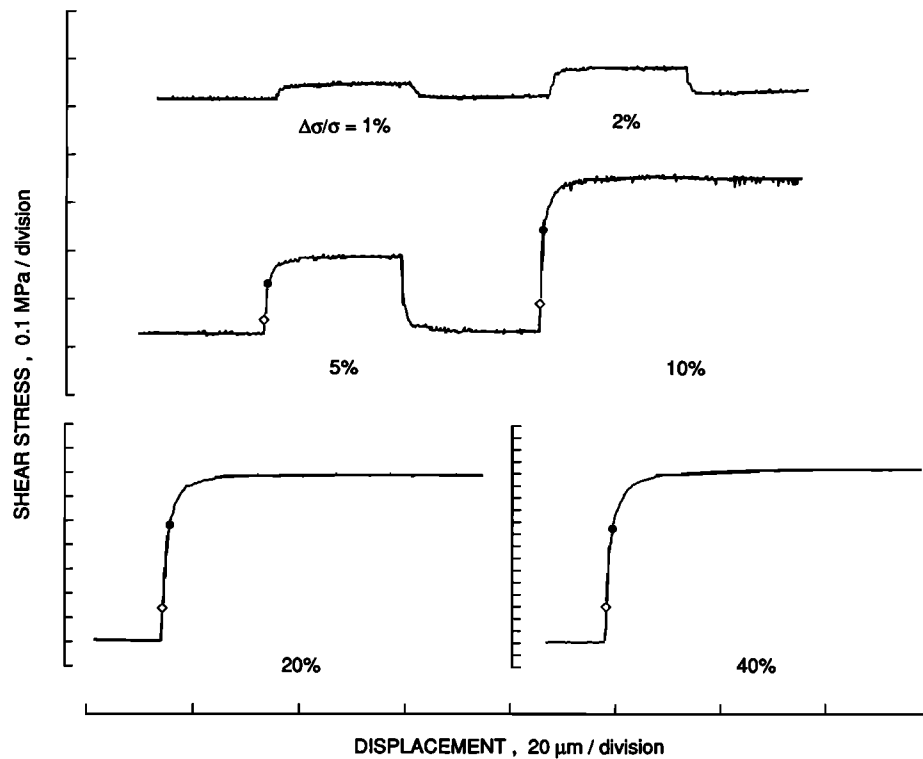


Fig. 3. Shear stress versus load point displacement for representative tests in which the normal stress is rapidly stepped while the load point displacement rate is held constant at $1 \mu\text{m/s}$. The magnitude of the normal stress changes are indicated in relation to the reference normal stress of 5 MPa. The diamonds represent the elastic response of shear stress to the imposed change in normal stress. The dots indicate the point at which the stress versus displacement curve departs from the elastic loading curve.

is not doubt less than the nominal rate so that our data are potentially affected by apparatus effects similar to those encountered by the previous workers. However, as we demonstrate later via numerical simulation, the small perturbations in slip rate that occur during our tests cannot account for the transient effects seen in the data.

Normal Stress Pulse Tests

With the normal stress pulse tests, the load point velocity is again held constant at $1 \mu\text{m/s}$ for the duration of the test. After reaching an initial steady state shear stress, the normal stress is briefly pulsed. The pulse consists of a rapid step up, followed shortly by a step down to the original normal stress. The commanded duration of each pulse is 200 ms. Upon completion of the stress pulse, sliding continues until the shear stress versus displacement curve becomes flat. At that point, another normal stress pulse is introduced. The amplitudes of the pulses range from 1 to 40% of the nominal 5.0-MPa normal stress, as in the normal stress step tests. Sequences of pulses conducted in the above manner with descending amplitude produce similar response to sequences with ascending pulse amplitude. Representative data are shown in Figure 4. At least two tests were performed for each pulse amplitude.

The immediate response of a normal stress pulse is a shear stress pulse, which occurs as the result of the previously noted elastic coupling of shear stress to normal stress. As expected, the amplitude of this pulse, which can be seen as spikes in Figure 4, scales linearly with the amplitude of the normal stress pulse, and the scale factor, $S \equiv \Delta\tau/\Delta\sigma$, is

about 0.2. Note also the correspondence between the amplitude of the spikes in Figure 4 and the diamonds in Figure 3. Following the normal stress pulse and accompanying shear stress pulse, the shear stress returns to roughly the initial steady state value, rises to a second peak, and then decays gradually to a steady state shear stress as sliding proceeds. The amplitude of the second peak in shear stress increases with the amplitude of the normal stress pulse, and the decay roughly follows an exponential with approximately the same characteristic displacement as for the normal stress step and velocity step tests. Again, compare the decay curves of Figures 4, 3, and 2.

Typically, the steady state shear stress following the decay is equal to the value prior to the normal stress pulse. The exceptions are tests in which the initial pulse amplitude is 40%. These tests often yield a final steady state shear stress that is greater than the initial steady state shear stress by about 0.6%. Curiously, repetitions of the 40% pulse consistently result in decays back to this new, slightly higher value of steady state shear stress.

We attribute the apparent increase in steady state shear stress following an initial, large normal stress pulse to friction within the sample assembly. The design of the sample assembly (Figure 1) allows the side blocks of the sample and the steel support blocks of the sample assembly to slide horizontally. Slip may occur on any of these horizontal surfaces in response to a change in horizontal load, if the frictional resistance is overcome. Consequently, if the sample assembly does not return to its initial configuration when the horizontal load is returned to its initial value, then

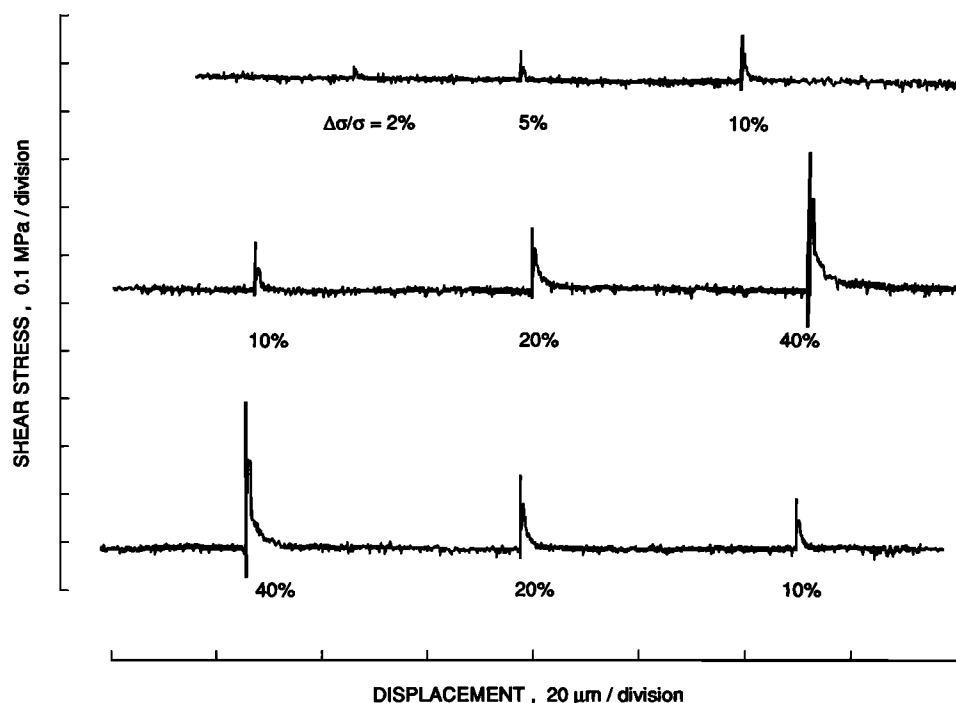


Fig. 4. Shear stress versus load point displacement for representative tests in which the normal stress is rapidly pulsed while the load point displacement rate is held constant at $1 \mu\text{m/s}$. The pulse consists of a rapid step up followed shortly by a rapid step down and has a duration of about 200 ms. The amplitude of the pulse is indicated in relation to the reference normal stress of 5 MPa. The sharp spikes in shear stress result from direct elastic coupling of shear stress to normal stress and correspond to the diamonds in Figure 3.

the normal stress on the rock to rock interface, following the pulse, will not return to its initial nominal value. The magnitude of this effect, as indicated by the 0.6% increase in steady state shear stress in response to the 40% pulse in horizontal load, is no more than about 0.6% of the normal stress or 0.03 MPa. We conclude that in the absence of such apparatus effects, a 40% pulse in normal stress would always result in a decay back to the initial steady state shear stress.

Summary of Normal Stress Step and Normal Stress Pulse Data

We have demonstrated that either a step or a pulse in normal stress produces a sudden change in shear strength and that, with continued sliding, the shear stress evolves toward a steady state value. In Figure 5 we have plotted the normalized change in shear strength that occurs during sliding, $\Delta\tau/\sigma_{\text{final}}$, versus a measure of the size of the normal stress perturbation. In the case of the normal stress step data, $\Delta\tau$ was obtained by estimating the point at which the shear stress versus load point displacement deviates from the elastic loading curve. Again, note the dots in Figure 3. Though there is some ambiguity in this picking procedure, we found that two observers would typically pick the same point to within about 6% of the total change in shear stress. For example, given a steady state coefficient of friction of 0.7, then in response to a 10% increase in normal stress from an initial normal stress of 5 MPa, the total change in shear stress is about 0.35 MPa, the portion of this change that occurs during sliding, $\Delta\tau$, is about 0.11 MPa, and the uncertainty in $\Delta\tau$ resulting from the ambiguity is about 0.02 MPa.

We represent the values of $\Delta\tau$ from the normal stress step tests, plotted in Figure 5, with the empirical relation

$$\frac{\Delta\tau}{\sigma} = \alpha \ln \left(\frac{\sigma}{\sigma_0} \right), \quad (8)$$

where σ_0 is the initial normal stress, σ is the final normal stress, $\Delta\tau$ is the amplitude of the change in shear stress that occurs during sliding, and α is a scale factor. The value of α , corresponding to the least squares fit line to the data in Figure 5, is 0.20. The ambiguity in the picking procedure introduces an uncertainty in the value of α of about 0.04. Upon inspecting Figure 5, one would conclude that the value of α , as defined by the procedure outlined here, is well constrained by the data. That is, the solid dots fall very close to the straight line. However, by including the effects of the finite load point stiffness in numerical simulations of these experiments, we will later demonstrate that our measurements of $\Delta\tau$ may be biased to the degree that this initial estimate of α is too small by more than a factor of 2.

5. PROPOSED CONSTITUTIVE LAW

Assumptions

In this section we develop a constitutive model to represent the changes in τ that result from changes in σ and V . Our proposed constitutive model extends the earlier model, summarized by equations (1) through (5), to incorporate the effects of changes in σ . For the purpose of our analysis, and for sufficiently small changes in normal stress, we assume that the steady state coefficient of friction is independent of

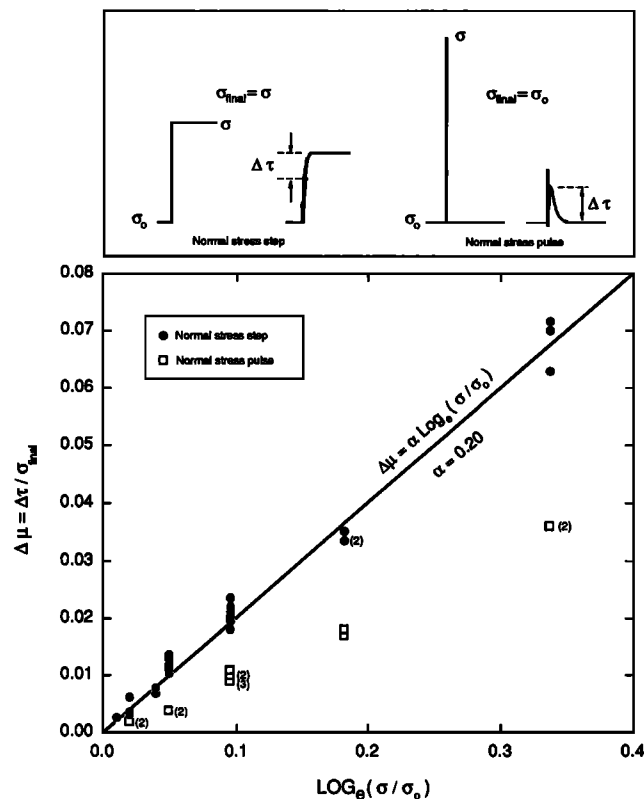


Fig. 5. The change in the coefficient of friction that occurs during sliding, following a perturbation in normal stress, is plotted versus the logarithm of the normalized amplitude of the perturbation. The initial normal stress is σ_0 , the maximum normal stress is σ , and the final normal stress is σ_{final} . The value of the change in the coefficient of friction represents the amplitude of the transient change in shear stress normalized by σ_{final} . Data from both the normal stress step tests (dots) and normal stress pulse tests (squares) are plotted. As in Figure 3, the dots correspond to the point at which the stress versus displacement curve departs from the elastic loading curve. The numbers 2 and 3 indicate the number of replicate measurements that plot at the position indicated in the figure. The line drawn through the data is the least squares fit to the normal stress step data, constrained to pass through the origin, and has a slope of 0.20.

normal stress. Furthermore, we assume that θ^{ss} is independent of normal stress. Consistent with the earlier model, we maintain the definition that $\theta^{ss} = D_c/V$. Thus implicit in our assumptions, we have assumed that D_c is also independent of normal stress. In addition, we assume that the constitutive parameters A and B , equation (3), are independent of normal stress for the range of normal stress examined here.

To represent the normal stress effects, we make the following three assumptions:

1. Changes in σ result in changes in state.
2. All state effects that result from changes in σ and from changes in V can be expressed by the state variable θ . This statement admits more than one characteristic displacement but only one functional dependence of θ on σ and V :

$$\frac{d\theta_i}{dt} = G(V, \sigma, \theta_i, D_c). \quad (9)$$

3. A sudden change in σ results in a sudden change in θ that is symmetric with regard to increases versus decreases in σ . For example, a pulse in normal stress of zero duration

would produce no net change in θ . These three assumptions form the simplest extension of the earlier constitutive model in which θ is determined by contact area [Dieterich, 1979a; Dieterich and Conrad, 1984].

Experimental Basis for the Proposed Constitutive Law

As described previously, the sudden increase in σ results in a sudden increase in τ followed by a further increase, in which τ asymptotically approaches a new steady state value as sliding proceeds. We have assumed that θ^{ss} is independent of normal stress and that $\theta^{ss} = D_c/V$. Therefore the evolution of state that occurs during sliding, following the increase in σ , must be toward the initial steady state value. We conclude that the sudden increase in σ must result in a sudden change in θ and that, with continued sliding at the higher normal stress, this change in θ is fully recovered as θ returns to θ^{ss} .

We define $\Delta\tau$ as the change in τ that occurs during sliding as the result of the sudden increase in σ . Using (3) and this definition of $\Delta\tau$, we obtain

$$\Delta\tau = B\sigma \ln\left(\frac{\theta^{ss}}{\theta}\right), \quad (10)$$

where θ is the value immediately following the step increase in normal stress, but prior to any sliding, and σ is the value following the step in normal stress. Earlier, we observed that $\Delta\tau$ can be represented empirically by (8). Substituting (8) for $\Delta\tau$ into (10) yields

$$\theta = \theta^{ss} \left(\frac{\sigma_0}{\sigma}\right)^{\alpha/B}. \quad (11)$$

Equation (11) gives the value of θ immediately following the rapid increase in normal stress, from σ_0 to σ . Since α is greater than B (Table 1), the effect of the step increase in σ is to suddenly decrease state from θ^{ss} to θ .

An Evolution Law for θ

Equation (11) was derived to represent the special case of a step increase in σ that occurs from steady state. We postulate that the form of equation (11) also holds for the more general case in which a step increase in σ occurs from an initial state θ_0 :

$$\theta = \theta_0 \left(\frac{\sigma_0}{\sigma}\right)^{\alpha/B}, \quad (12)$$

where θ_0 is the value prior to an increase in normal stress from σ_0 to σ and θ is the value immediately following the change in σ . We postulate further that (12) also applies to a decrease in normal stress where σ is less than σ_0 .

According to our proposition, the value of θ immediately following a rapid, finite change in σ is given by equation (12). Differentiating (12), we obtain the general expression that governs the evolution of θ in response to a change in σ :

$$\left(\frac{\partial\theta}{\partial\sigma}\right)_{\delta = \text{const}} = -\left(\frac{\alpha\theta}{B\sigma}\right), \quad (13)$$

where θ and σ correspond to the values immediately following a rapid change in σ . By combining (13) with an expression that governs the evolution of θ in response to slip, or a change in slip rate, we obtain the governing equation for the evolution of θ applicable to conditions of variable σ and V :

$$d\theta = \left(\frac{\partial \theta}{\partial \delta} \right)_{\sigma = \text{const}} d\delta - \left(\frac{\alpha \theta}{B\sigma} \right) d\sigma. \quad (14)$$

Equations (4) and (5) are two particular examples of $(\partial \theta / \partial \delta)_{\sigma = \text{const}}$. In the following, the use of equation (4) in (14) is referred to as evolution law 1, and use of equation (5) in (14) is referred to as evolution law 2.

Equation (14) forms the principal product of this study. It is our proposed expression for how state varies under conditions of variable slip rate and normal stress. In Appendix B we discuss our physical interpretation of state under such conditions.

6. TESTS OF THE PROPOSED CONSTITUTIVE LAW

We test our proposed constitutive law by comparing model predictions with the data. The comparisons allow us to test two of our propositions: (1) the state variable θ is sufficient to represent the variation in τ that results from changes in both slip rate and normal stress, and (2) from a general state θ_0 , the sudden change in θ that results from a change in σ can be represented by (12).

The model predictions are generated by numerical simulations, which incorporate the proposed constitutive law and include the mechanical effects of the double direct shear apparatus. Initially, we consider whether the effects that we have ascribed to a dependence of θ on σ could be attributed solely to slip rate effects. Next, we analyze the relatively simple normal stress step test and then the somewhat more complicated normal stress pulse test. Finally, we analyze data from the, yet to be presented, hold-pulse tests, which severely test the proposed constitutive model by intentionally varying both normal stress and slip rate.

Numerical Method

The numerical model employs the proposed constitutive relations, equations (3) and (14), and represents apparatus interactions as a simple spring and slider system with coupling of shear stress to normal stress as described below. In this system, motion of the load point corresponds to the point at which displacements are sensed for servo-control, and the spring represents the shear stiffness K of the sample assembly between the displacement sensing point and the sliding surfaces. The applied shear stress τ is

$$\tau = K(d_l - \delta), \quad (15)$$

where d_l is the displacement of the load point and δ is the displacement of the slider. The appropriate stiffness for the simulations was measured from experimental loading curves where it was found to be 0.5 ± 0.1 MPa/ μm . For these simulations we have not included the time response of the servo-control systems for either load point or normal stress control. Rather, the displacement of the load point follows the prescribed history, and changes in normal stress are applied directly to the slider.

To represent the elastic coupling of shear stress to normal

stress observed in the normal stress step experiments (Figure 3), and more dramatically in the normal stress pulse experiments (Figure 4), a similar coupling of shear stress to imposed normal stress is included in the model:

$$S\Delta\sigma \Rightarrow \Delta\tau, \quad (16)$$

where $\Delta\tau$ is the immediate change of shear stress resulting from an imposed change in normal stress $\Delta\sigma$. The factor S is about 0.2 in our experiments. Recall that the coupling of shear stress to changes in normal stress occurs because the vertical ram is servo-controlled in relation to the load point displacement, not in relation to either slip or shear stress. Since the horizontal ram is controlled in relation to load, there is not a comparable coupling of normal stress to changes in shear stress.

Motion of the slider and the corresponding shear stress are the quantities to be determined. The simulations employ a time-marching procedure that assumes constant slip speed and constant normal stress during a time step. Steps in σ required by the simulations occur instantaneously between the time steps. The calculation of unknown slip speed requires that, at the midpoint of the step, the frictional resistance τ_f is equal to the applied stress τ_e . The slip speed that satisfies this condition is iteratively determined using a predictor-corrector method. Each iteration begins with a trial τ_f^i , where i indicates the i th iteration. The first iteration begins with τ_f^1 set equal to the known stress at the beginning of the step. The trial slip speed V_{trial} that yields a frictional resistance equal to τ_f^i at the midpoint of the step is calculated from the constitutive relations. This calculation employs the explicit $V = \text{const}$, $\sigma = \text{const}$ solution of the evolution equations to evolve θ through the time step, as given by equations (6) and (7) for evolution law 1 and evolution law 2, respectively. The spring distortion and corresponding elastic stress at the midpoint, τ_e^i , are then calculated using V_{trial} . If $|\tau_f^i - \tau_e^i| \geq \tau_{\text{error}}$, then another iteration is performed using $\tau_f^{i+1} = \tau_e^i$.

This method is numerically stable for step sizes as large as $0.1D_c$ and is relatively easy to implement. For the simulations reported here, $\tau_{\text{error}} = 10^{-4}\sigma$ and the time step solution generally converges after three iterations or less. The solutions are insensitive to the size of the steps, provided $\Delta\delta \leq 0.05D_c$ and provided $\Delta d_l \leq 0.05D_c$. In the simulations reported below, the steps were adjusted such that $\Delta\delta \leq 0.02D_c$ and $\Delta d_l \leq 0.02D_c$.

The constitutive and model parameters used for the following simulations are listed in Table 1 and were determined, by trial and error, to give the most satisfactory fit to all of the experiments. Though the optimal parameter values differ for the two evolution laws, all are in rough agreement with the values determined directly from the data, with the exception of α . Determination of α is discussed below.

Confirmation of State Dependence on Normal Stress History

First we test whether the effects that we have ascribed to a dependence of state on normal stress history could be caused solely by perturbation of slip rate arising from finite load point stiffness. We test this hypothesis by performing simulations of the normal stress step and normal stress pulse experiments assuming no dependence of state on normal stress history, i.e., $\alpha = 0$.

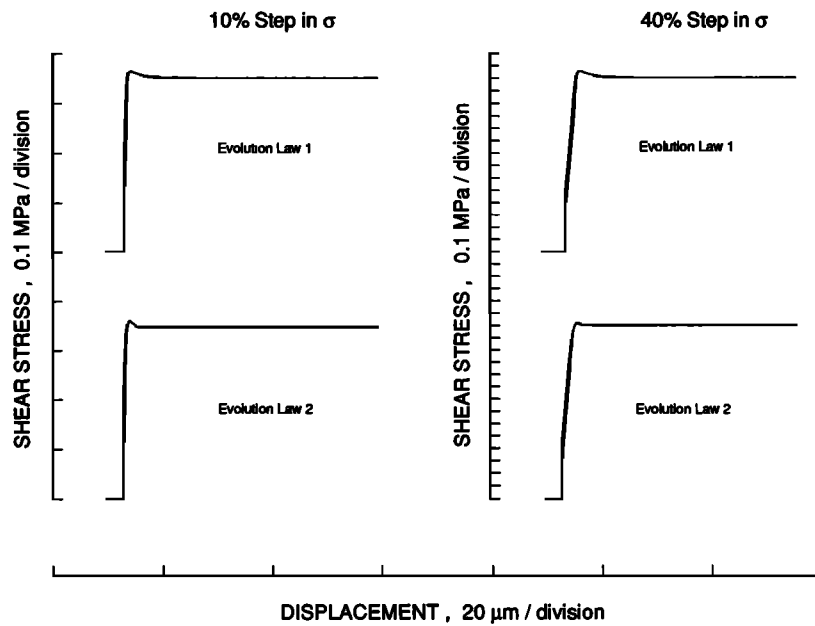
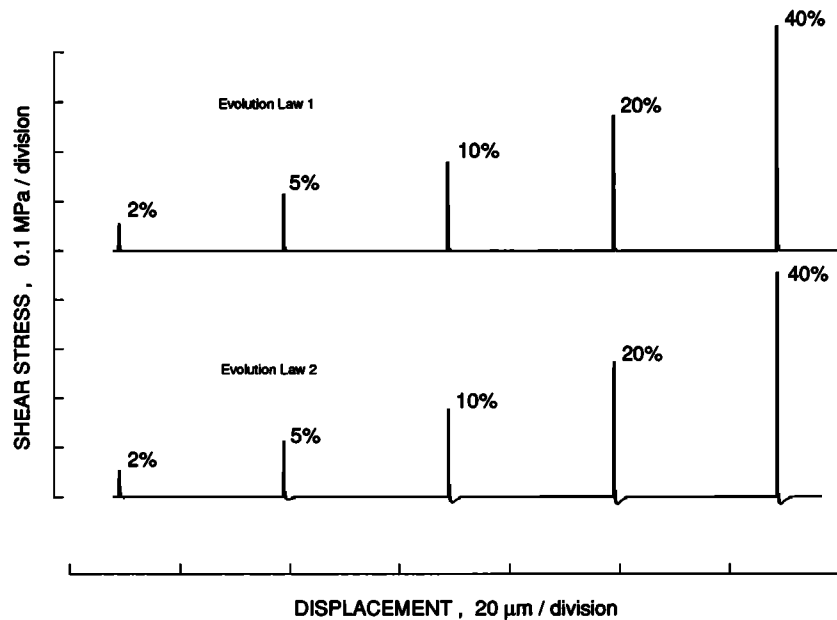
a) SIMULATION OF NORMAL STRESS STEP TEST WITH $\alpha = 0$ b) SIMULATION OF NORMAL STRESS PULSE TEST WITH $\alpha = 0$ 

Fig. 6. Simulations of (a) normal stress step experiments and (b) normal stress pulse experiments, using the parameter values listed in Table 1 but with the parameter α set to zero and employing evolution laws 1 and 2, respectively. Unlike the data in Figure 3, simulations of the step experiments result in a shear stress overshoot following the step increase in normal stress. Simulations of the pulse tests do yield the elastic coupling of shear stress to normal stress that is seen in the data (Figure 4) but do not yield the observed transient change in shear stress that occurs during sliding. The failure of these simulations to match the principal features of our data demonstrates that the observed effects of variable normal stress are not due solely to slip rate effects, which act through the finite load point stiffness of the apparatus, but rather that the state variable depends on normal stress history.

Examples of normal stress step and normal stress pulse simulations with $\alpha = 0$, but with all other parameters as listed in Table 1, are shown in Figure 6. The simulations of the normal stress step test with $\alpha = 0$, Figure 6a, result in a transient peak in shear stress and subsequent decay to the

steady state value in response to a step increase in normal stress while the data, Figure 3, reveal a monotonic rise in shear stress toward the steady state value. The simulations of the pulse tests with $\alpha = 0$, Figure 6b, fail to show the postpulse peak in shear stress that is seen in the data, Figure

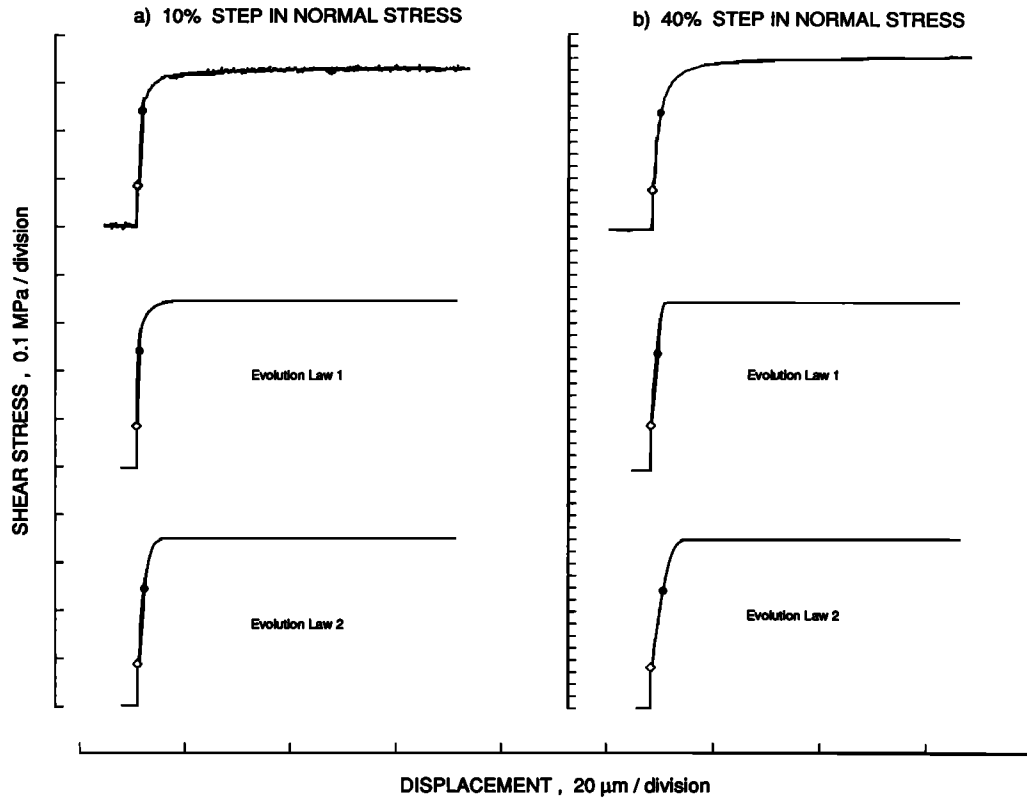


Fig. 7. Data and simulations from normal stress step tests. The simulations use the parameter values listed in Table 1. On the experimental records, the dots indicate the value $\Delta\tau$ used to produce Figure 5. Similarly, on the simulations, the dots denote the value of $\Delta\tau$ corresponding to the value of α , 0.20, derived from the least squares fit to the data in Figure 5. For the most part, the dots appear to mark adequately the point at which the shear stress paths depart from the linear portion of the curves even though the value of α used in the simulations with evolution law 2 employed $\alpha = 0.56$. The exception is the 40% step using evolution law 1. The diamonds represent the elastic coupling of shear stress to normal stress, as in Figure 3.

4. The inability of these simulations to match the data is a demonstration that the perturbation of slip rate, which occurs in our experiments, cannot alone account for the data. Therefore the transient effects observed in our data must be due, at least in part, to a dependence of state on normal stress history.

Normal Stress Step and Normal Stress Pulse Experiments

The normal stress step experiment is relatively simple in that it involves only a single, sudden change in normal stress and thus only a single sudden perturbation of θ from its initial value, θ^{ss} . In contrast, the pulse experiment is a more severe test of the constitutive model, since there a second sudden change in θ occurs at a time when θ is not at steady state. During the pulse experiment, θ first decreases from its initial value, θ^{ss} , in response to the step increase in normal stress, just as in the step experiment, according to equation (11). Then, during the brief 0.2-s interval between the step up and the step down in normal stress, θ evolves toward steady state, again, just as in the step experiment. Next, according to the proposed constitutive law, θ increases suddenly in response to the downward step in normal stress, by an amount equal and opposite to the previous sudden change in θ , even though this second sudden change in θ takes place from a value other than θ^{ss} . This symmetric response of θ to a decrease in normal stress relative to an increase in normal

stress, at a time when θ is not equal to θ^{ss} , is the assumption of equation (12). Notice that under this assumption, if the pulse had zero duration and the amount of slip that occurred during the pulse was also zero, then the net change in θ in response to a pulse would be zero so that a pulse in normal stress would yield no transient change in shear stress.

We compare data from normal stress step tests to simulations using the two evolution laws, 1 and 2, and the corresponding best values of α , 0.23 and 0.56, respectively (Figure 7). The value of α estimated directly from the experimental curves, 0.20, is reasonably close to the preferred value determined in the simulations using evolution law 1, 0.23, but differs by more than a factor of 2 from the value of 0.56 determined using evolution law 2. The diamonds on the curves in Figure 7 indicate the immediate jump in shear stress due to the elastic stress coupling effect. The dot on the two experimental curves marks the stress that was picked to produce the data in Figure 5 and the corresponding value of α , 0.20. Likewise, the dots on the simulations correspond to the linear fit to the data in Figure 5, $\alpha = 0.20$, and in most cases adequately mark the point at which the stress-displacement curves begin to deviate from the linear trend. Therefore our picking procedure, if applied blindly to the stress-displacement records produced by the simulations, would yield a value of α about equal to 0.20 even though the simulations employing evolution law 2 used $\alpha = 0.56$. This discrepancy between the picked value of α , 0.20,

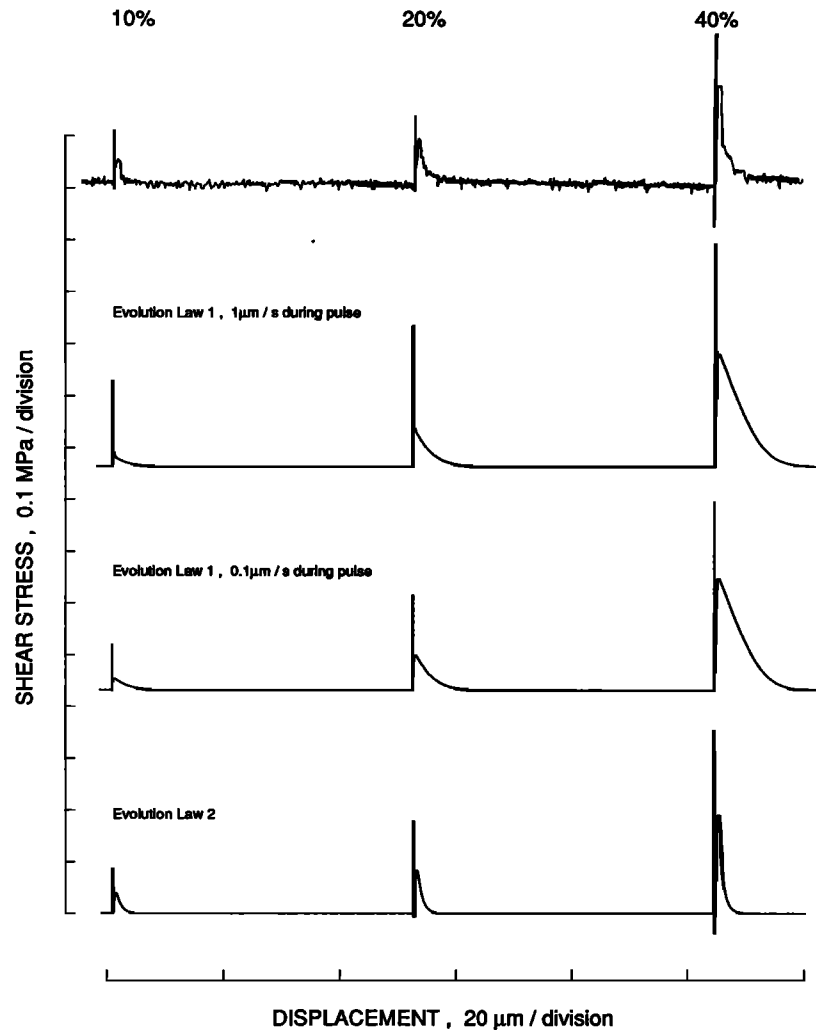


Fig. 8. Data and simulations from normal stress pulse tests. The top curve is data. The lower three curves are simulations. The simulations use the parameter values listed in Table 1. In each of the simulations, a shear stress spike results from elastic coupling of shear stress to normal stress, and its amplitude corresponds to the diamonds in Figure 7. The first simulation uses evolution law 1 and the nominal load point speed of $1.0 \mu\text{m/s}$. In the resulting curves the shear stress transient has merged with the spike that results from the elastic coupling of shear stress to normal stress. The second simulation uses evolution law 1 and a load point speed of $0.1 \mu\text{m/s}$. The choice of $0.1 \mu\text{m/s}$ is ad hoc but does produce curves that look much like the data. The last simulation uses evolution law 2 and the nominal load point slip speed of $1 \mu\text{m/s}$ and appears to match the data adequately.

and the value that best simulates the data when using evolution law 2, 0.56, results from the complex interaction of the load point and the sliding surface. One lesson to be learned here is that only by performing numerical simulations, which adequately model the interaction between the apparatus and the specimen, are we able to draw reliable conclusions from our friction data. We conclude that the normal stress step test does not provide an accurate measure of α if indeed evolution law 2 applies.

The one exception to the general pattern of agreement between the simulations and the data from the normal stress step tests displayed in Figure 7 is the case of evolution law 1 for the 40% step in normal stress; see Figure 7*b*. For this one case the knee in the curve is very abrupt, i.e., the apparent decay distance is very short, and the dot corresponding to $\alpha = 0.20$ grossly misses the departure of the shear stress path from the elastic loading curve. We have no explanation for this discrepancy.

Next, we compare simulated and observed shear stress

versus displacement curves for the normal stress pulse experiments (Figure 8). In each of the simulations, a shear stress spike results from the elastic stress coupling effect and its amplitude corresponds to the diamonds in Figure 7. Two different simulations are shown using evolution law 1. In the first the velocity of the load point is maintained at the nominal experimental rate of $1.0 \mu\text{m/s}$, while in the second the load point velocity during the pulse is assumed to be $0.1 \mu\text{m/s}$. In the first case the shear stress transient that occurs following the normal stress pulse merges with the shear stress spike that results from the stress coupling effect. This merging is not seen in the data. In addition, the amplitudes of the shear stress transients, corresponding to the normal stress pulses of 2%, 5%, and 10%, significantly exceed the observed values. In the second case, where the load point velocity during the pulse is assumed to be $0.1 \mu\text{m/s}$, the simulations appear more like the data. That is, the shear stress transient following the normal stress pulse does not merge with the shear stress spike, and furthermore, the

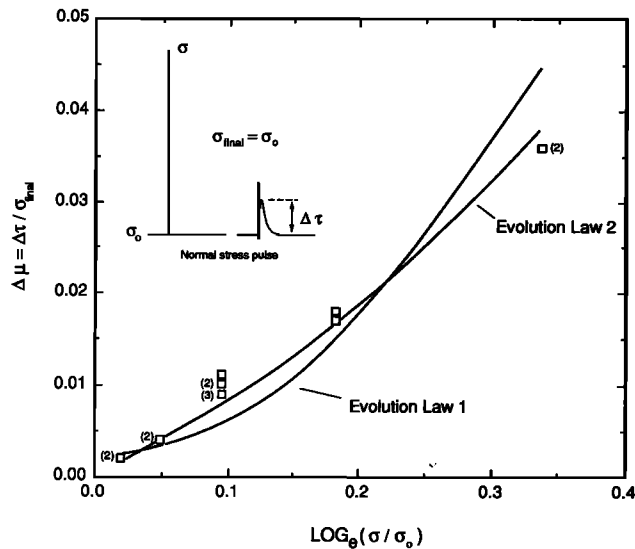


Fig. 9. The change in the coefficient of friction that occurs during sliding, following a pulse in normal stress, is plotted versus the logarithm of the normalized amplitude of the pulse. As in Figure 5, the value of the change in the coefficient of friction represents the amplitude of the transient change in shear stress normalized by the final normal stress, σ_{final} . The data are taken from Figure 5. The curves represent simulations of pulse tests using the two evolution laws and the parameter values listed in Table 1. A load point velocity of $0.1 \mu\text{m/s}$ is assumed during the pulse for the simulations using evolution law 1, while those using evolution law 2 use the nominal $1.0 \mu\text{m/s}$.

amplitudes of the shear stress transients are comparable to those from the experiments. The use of $0.1 \mu\text{m/s}$ for the load point velocity is ad hoc but motivated by the possibility that the response of the servo-control may be too slow to maintain the load point velocity at the desired rate during the 0.2-s pulse. Unfortunately, we have no independent measure of load point velocity during a pulse with which to test this hypothesis. In the third simulation, where evolution law 2 is used (Figure 8), no adjustment of the load point velocity is required to provide an acceptable representation of the experimental curves.

The amplitude of the shear stress transients that were generated by simulation of the normal stress pulse tests is compared with the experimental results in Figure 9. The simulations with evolution law 1 use a load point velocity of $0.1 \mu\text{m/s}$ during the pulse, while those with evolution law 2 use the nominal $1.0 \mu\text{m/s}$. While the simulations using either evolution law are in rough agreement with the data, evolution law 2 appears to be superior, especially for large normal stress pulses.

In summary, we have tested the proposed constitutive model against our observations from the normal stress step experiments and the normal stress pulse experiments. We conclude that the assumptions required to obtain equation (12) from equation (11) are supported by the data from the pulse tests. Our simulations of the relatively simple step experiment appear to adequately represent the experimental data with the exception of the 40% steps using evolution law 1. The constitutive model also appears capable of characterizing the observations from the more severe normal stress pulse tests. Here again, however, the validity of evolution law 1 appears somewhat questionable because of the exper-

imentally unsubstantiated need to alter load point displacement rates during the normal stress pulse.

The Hold-Pulse Tests

As a further and yet more rigorous test of the constitutive model, we have conducted experiments in which both normal stress and load point velocity are varied. In these tests, the normal stress is briefly pulsed while the load point is held stationary for a measured duration. Then, following the hold, the load point displacement is resumed at the initial, nominal rate. We refer to these experiments as "hold-pulse" tests. As in our previous tests, the nominal load point displacement rate is $1.0 \mu\text{m/s}$, and the reference normal stress is 5.0 MPa . The duration of the hold is measured from the cessation of the load point displacement. The pulse in normal stress, imposed 0.1 s after initiation of the hold, is identical to those imposed in the normal stress pulse tests, where the commanded duration of the pulse is 0.2 s.

Dieterich [1981] performed analogous tests in which the normal stress remained constant during the experiment. Our tests conducted with zero-amplitude normal stress pulse are identical to Dieterich's so-called "hold tests." As we have shown, a pulse in normal stress yields a value of state θ_0 that is different from θ^{ss} . Likewise, in a hold-pulse test the evolution of θ that occurs following the pulse in normal stress, but during the load point hold, begins from the non-steady-state value, θ_0 , resulting from the pulse. Consequently, the hold-pulse experiment severely tests both the normal stress term as well as the slip rate term of the general evolution law given by equation (14).

Figure 10 compares simulations and data for three hold-pulse tests, each with the duration of the load point hold equal to 1 s. In the first test the normal stress is held constant, while in the second and third tests the normal stress is pulsed by 20% and by 40% above 5 MPa, respectively. The constitutive parameters used in the simulations, and listed in Table 1, are those that simultaneously best represent all of our experiments, namely, velocity steps, normal stress steps, normal stress pulses, and hold-pulse tests. As seen in the figure, the pulse in normal stress produces a spike in shear stress that is equivalent to those that occur in the normal stress pulse test and which result from the previously described coupling of shear stress to normal stress. Next, the shear stress relaxes during the hold as the slider continues to move, at rates that decrease with time. Upon resumption of displacement of the load point, the shear stress passes through a transient peak, $\Delta\tau$, as defined in the figure. For the 1-s holds, the effect of the pulse in normal stress is to increase $\Delta\tau$ by an amount that increases with the amplitude of the pulse.

The results of our hold-pulse experiments and the corresponding simulations are summarized in Figure 11, where $\Delta\tau$ is plotted for the three pulse amplitudes 0%, 20%, and 40% of 5 MPa and hold times of 0.1 to 10,000 s. Our data from zero-amplitude normal stress pulses reveal the same general features seen in previous hold tests [see Dieterich, 1981, Figure 10]. In particular, for long hold times, $\Delta\tau$ increases approximately linearly with the logarithm of the duration of the hold. According to the constitutive law, θ increases during the hold while the slider creeps and the load relaxes. At the end of the hold period, θ has obtained a value that exceeds $\theta^{ss} = D_c/V$, where V is the nominal slip speed. It

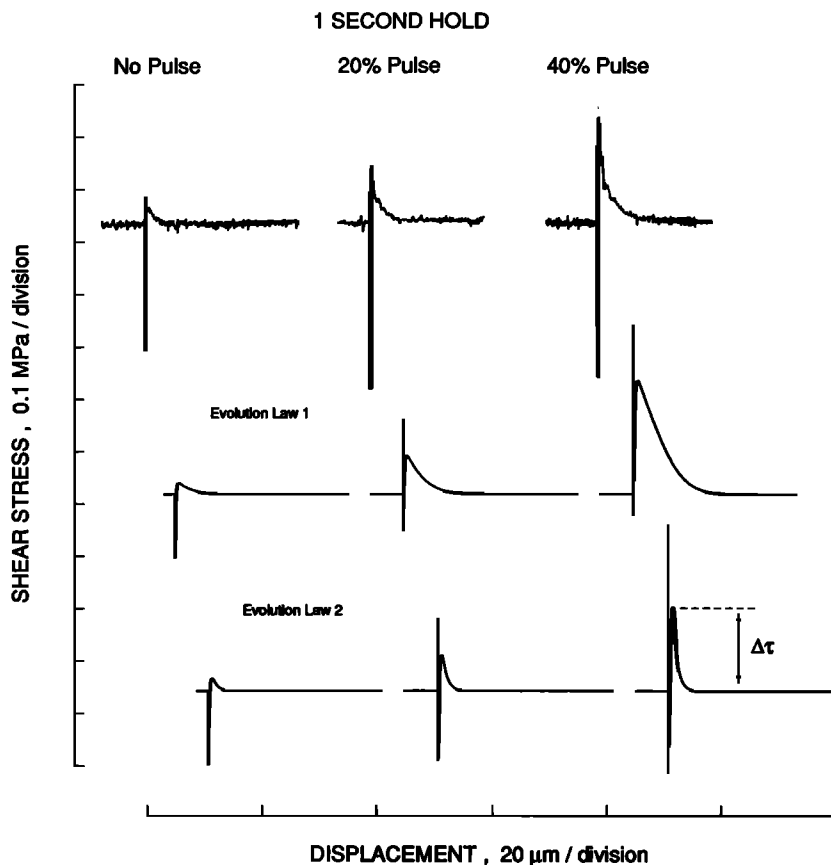


Fig. 10. Data and simulations of hold-pulse tests with 1-s holds. In hold-pulse tests, the load point is stopped for a measured duration before displacement is resumed at the initial rate of 1 $\mu\text{m/s}$. At 0.1 s into the load point hold, the normal stress is pulsed, exactly as in the pulse tests. Upon the resumption of sliding, the shear stress rises through a transient of amplitude $\Delta\tau$. The simulations use evolution laws 1 and 2 and the parameter values listed in Table 1.

is this increase in θ that results in the observed transient increase in shear stress, $\Delta\tau$.

The introduction of a normal stress pulse during a load point hold can be examined, again by studying Figure 11.

For the shorter hold times the effect of a normal stress pulse is to increase the height of the friction transient, $\Delta\tau$, by an amount that is relatively insensitive to the duration of the hold. In the limiting case of no load point hold, a hold-pulse

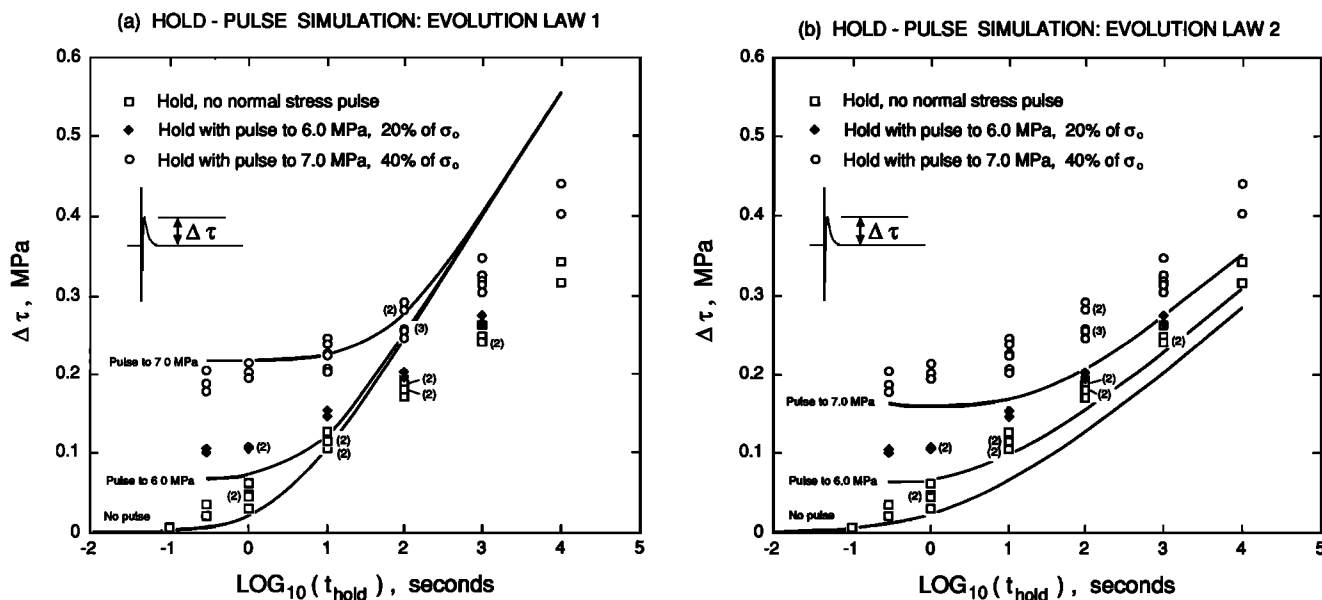


Fig. 11. The shear stress transient that results from the hold-pulse tests is plotted versus the logarithm of the duration of the hold. Data from pulses of 0, 20, and 40% of 5 MPa are shown by boxes, diamonds, and circles, respectively. The curves represent simulations of hold-pulse tests using (a) evolution law 1 and (b) evolution law 2 and the parameter values listed in Table 1.

test is equivalent to a normal stress pulse test. Thus according to our proposed model the variation of $\Delta\tau$ with pulse amplitude, as plotted near the left edge of the figure, is determined primarily by the value of α . At long hold times the effect of the pulse is less pronounced and $\Delta\tau$ again increases in approximate proportion to the logarithm of the hold time.

The curves plotted in Figure 11a and 11b represent simulations of hold-pulse tests employing evolution law 1 and evolution law 2, respectively. The model parameters are, again, those listed in Table 1 and are those that best represent the data from all of our tests. As can be seen in the figure, both evolution laws give general qualitative agreement with the data. That is, both reveal that at short hold times $\Delta\tau$ increases with the amplitude of the pulse in normal stress, and $\Delta\tau$ is relatively insensitive to the duration of the hold. In addition, at long hold times, $\Delta\tau$ increases approximately linearly with the logarithm of the duration of the hold. In detail, however, neither set of model predictions agree with the data. For example, at long hold times, the simulations using evolution law 1 overpredict the rate of increase of $\Delta\tau$ as a function of hold time. Likewise, the simulations using evolution law 2 produce curves that appear to be shifted to the right relative to the data.

In analyzing the data from his hold tests, Dieterich [1981] performed numerical simulations employing the same evolution laws that we have adopted here, but for the special case of constant normal stress, and noted similar discrepancies between his model and the data. The principal discrepancies between the simulations and the data can be associated with two of the parameters in the model, namely, B and D_c . In Figure 11a the slope of the curves at long hold times is determined by the value of B . In Figure 11b the horizontal position of the bend in the curves is determined by the value of D_c . Therefore one way around these discrepancies would be to choose values of B and D_c that produce curves in Figures 11a and 11b that match the hold-pulse data. Instead, we have chosen to consider all of our data in constraining the values of the parameters used in the simulation rather than adopting different parameter values for each different experiment. In particular, the values of both B and D_c are constrained by the data from the velocity stepping tests. The parameter B represents the amplitude of the decay in shear stress that follows a change in slip speed, while D_c represents the characteristic displacement of the decay in shear stress following the velocity step (Figure 2). To match the current model to the hold-pulse data in Figure 11a would require the adoption of a value of B less than the value that is consistent with the velocity step data by about a factor of 2. Likewise, to match the current model to the hold-pulse data in Figure 11b would require the adoption of a value of D_c less than the value that is consistent with the velocity step data by about a factor of 5.

An alternative resolution to the discrepancies between the model predictions and the hold-pulse data is to include a second state variable that obeys the previously employed evolution laws but operates over a different characteristic displacement. By including a second state variable in this manner, one introduces two additional parameters into the model. Instead of one value of D_c and one value of B , two characteristic displacements and two values of B , each associated with a particular value of D_c , are included. The incorporation of two characteristic displacements is sup-

ported by the shape of the decay curves from the velocity stepping tests (Figure 2). In detail, those decay curves show a rapidly evolving transient that immediately follows the step in slip speed, indicative of a small D_c , while at the larger displacements, there is a persistent slow change of shear stress characteristic of large D_c . Other workers have, in fact, argued that the data from their velocity stepping tests require two characteristic displacements [Ruina, 1980, 1983; Weeks and Tullis, 1985; Tullis and Weeks, 1986]. In principle, by choosing the appropriate values of the B_i , whose sum now represents the amplitude of the decay in shear stress that follows a change in slip speed, and the appropriate values of D_c one could match the data from the hold-pulse tests in Figures 11a and 11b while still satisfying the data from the velocity stepping tests. We have chosen not to include this degree of complexity, or perhaps refinement, in our model.

7. DISCUSSION

We have observed that normal stress history significantly affects the coefficient of friction for one rock type at one normal stress and one slip rate, specifically Westerly granite at a normal stress of 5 MPa and a slip rate of 1 $\mu\text{m/s}$. However, the work of previous investigators, while not duplicating our experiments, does indicate the same general features that we have observed in our normal stress stepping tests and suggests some general validity of our proposed constitutive law. For example, the experiments of Hobbs and Brady [1985] were conducted on gabbro, the experiments of Lockner *et al.* [1986] were conducted on Westerly granite with a layer of gouge, and the experiments of Olsson [1988] were conducted on welded tuff. Lockner *et al.*'s experiments were performed at a normal stress of 50 MPa, while those of Olsson were performed at 2 to 6 MPa. We are encouraged that the state variable formulation not only appears to apply to a wide range of rock types at constant normal stress, but also that the effects of variable normal stress appear to be characterized by our proposed model.

The data that we have presented represent the variation in the resistance to sliding that results from relatively small changes in normal stress. We suspect that for sufficiently large changes in normal stress, the effects on θ , as outlined here, may saturate. A saturation effect could be incorporated into our model by the inclusion of suitable cutoff parameters [see Dieterich, 1979a, 1981; Okubo and Dieterich, 1986]. We also recognize that the steady state coefficient of friction may have a weak dependence on normal stress [Byerlee, 1978] that is not included in our model.

As discussed in the introduction, our results may have application when considering other laboratory experiments or faults in nature where normal stresses are generally not constant. Because normal stress effects can mimic slip rate effects, the interpretation of laboratory data can be complicated. We have addressed this complication by performing numerical simulations that attempt to characterize the interaction of our testing machine and the specimen. Similar numerical simulations could also be performed for other experimental configurations, though the characterization of other apparatus may be more complicated than for the double direct shear apparatus and thus less well constrained.

Olsson [1988], for example, performed tests in which the normal stress was increased at a constant rate while load

point speed was held constant. We have not performed normal stress ramping experiments, nor have we performed such simulations, but we expect that our proposed constitutive model could adequately simulate most of the effects reported by Olsson. We suggest that such simulations be performed in the future.

Perhaps the most important question regarding the effects of variable normal stress is how they may affect the stability of a frictional system. Under conditions of constant normal stress, instability is promoted by large $B - A$, small D_c , and low stiffness [Dieterich, 1978; Ruina, 1980, 1983; Rice and Ruina, 1983; Gu et al., 1984]. There is no doubt that decreases in normal stress also promote instability, and our data indicate that the onset of instability will be influenced through the effect of normal stress on θ . For example, in response to a sudden decrease in normal stress, the shear strength drops suddenly by an amount that is controlled by the parameter α and then continues to decrease toward the new steady state shear stress as sliding proceeds. Thus we may conclude that the parameter α will influence stability. Stability analyses that investigate the effects of both variable normal stress and variable slip rate, as incorporated by our model, are planned.

Olsson [1988] presented a constitutive law based on classical viscoelasticity with a hereditary integral to accompany the data from his variable normal stress experiments. In contrast to the constitutive law that we have proposed, his law does not include a weakening distance, and so it is unlikely to be capable of reproducing all of the effects that we have observed. This assertion should be tested in future work.

The effects of variable normal stress in the Earth could be incorporated in many analyses by utilizing our model. One area of study is given by large-scale faulting where normal stress will vary because of nonplanar fault geometry, en echelon steps, and slip on adjacent faults. A particular example, which we mentioned in the introduction, is the effort to understand how the stress changes associated with the May 1983 Coalinga earthquake were related to the observed changes in creep rate along the San Andreas fault [Mavko et al., 1985]. In spite of the fact that the calculated coseismic changes in normal traction on the San Andreas fault exceeded the changes in shear traction by at least a factor of 2, Simpson et al. [1988] developed a model in which the shallow region of the fault zone responds only to changes in shear stress. Their model produced changes in creep rates of the correct sense, but not of the correct magnitude. We expect that a model that is sensitive not only to changes in shear stress but also to changes in normal stress might provide additional insight into how the San Andreas fault responds to sudden changes in stress such as that imposed by the Coalinga earthquake.

8. CONCLUSIONS

1. A sudden change in normal stress results in both a sudden and a transient change in the resistance to sliding.
2. The coefficient of friction depends on slip speed and a parameter representing the state of the sliding surface. The state of the sliding surface depends both on prior slip speed and on prior normal stress.
3. The functional dependence of state on normal stress can be expressed in terms of the same state variable, θ ,

previously used to represent slip rate history effects. The variable θ has the interpretation of effective contact time. We assume that the steady state value of θ is independent of normal stress and that $\theta^{ss} = D_c/V$.

4. At constant slip speed and from an initial steady state, a sudden change in normal stress results in a sudden change in θ , followed by a gradual change in θ toward θ^{ss} as sliding proceeds.

5. The sudden change in θ that results from a change in normal stress is determined by a newly identified parameter, which we call α .

6. Stability will be influenced by $B - A$, stiffness, D_c , α , slip rate history, and normal stress history.

APPENDIX A: ALTERNATIVE FORMULATION FOR THE CONSTITUTIVE LAW

Here we present the constitutive relations representing the variation in friction that results from changes in slip rate and normal stress, equations (3)–(7) and (13)–(14), in terms of an alternate representation of state that was originally introduced by Ruina [1980, 1983] and later adopted by other workers. Instead of employing the state variable θ , Ruina defines a related state variable Θ :

$$\Theta = \ln(\theta/\theta^*). \quad (17)$$

Substituting (17) into the constitutive law, equation (3), yields

$$\tau = \mu^* \sigma + A \sigma \ln(V/V^*) + B \sigma \Theta. \quad (18)$$

In some studies the term B has been absorbed into the definition of Θ .

Recall from (3) that θ^* and V^* are defined for steady state slip such that when $V = V^*$, $\theta^{ss} = \theta^*$. Hence from the definition of steady state, $\theta^{ss} = D_c/V$, we must have that

$$\theta^* = D_c/V^*. \quad (19)$$

In terms of Θ , evolution law 1 for slip at constant normal stress, equation (4), becomes

$$\left(\frac{\partial \Theta}{\partial \delta}\right)_{\sigma = \text{const}} = \frac{1}{V} \left(\frac{\partial \Theta}{\partial t}\right)_{\sigma = \text{const}} = \frac{V^*}{VD_c \exp(\Theta)} - \frac{1}{D_c}. \quad (20)$$

At constant slip speed, (20) has the solution corresponding to (6):

$$\Theta = \ln \left\{ \frac{V^*}{V} + \left[\exp(\Theta_0) - \frac{V^*}{V} \right] \exp[(\delta_0 - \delta)/D_c] \right\}, \quad (21)$$

$$V = \text{const}$$

Substitution of (17) and (19) into evolution law 2, equation (5), yields

$$\begin{aligned} \left(\frac{\partial \Theta}{\partial \delta}\right)_{\sigma = \text{const}} &= \frac{1}{V} \left(\frac{\partial \Theta}{\partial t}\right)_{\sigma = \text{const}} \\ &= -\left(\frac{1}{D_c}\right) \left[\Theta + \ln\left(\frac{V}{V^*}\right) \right], \end{aligned} \quad (22)$$

which has the constant slip speed solution corresponding to equation (7):

$$\Theta = \ln \frac{V^*}{V} + \left(\ln \frac{V}{V^*} + \Theta_0 \right) \exp [(\delta_0 - \delta)/D_c], \quad (23)$$

$$V = \text{const}$$

Rice and Tse [1986] have combined (18) and (22) to eliminate the explicit appearance of Θ .

In terms of Θ , the change of state in response to a step change in normal stress from σ_0 to σ , equation (12), becomes

$$\Theta = \Theta_0 + \frac{\alpha}{B} \ln \left(\frac{\sigma_0}{\sigma} \right). \quad (24)$$

Finally, the general evolution equation (14) is given by

$$d\Theta = \left(\frac{\partial \Theta}{\partial \delta} \right)_{\sigma = \text{const}} d\delta - \left[\frac{\alpha}{B\sigma} \right] d\sigma. \quad (25)$$

With Θ , the expressions for evolution law 2 are somewhat simplified; compare equations (5) and (7) with equations (22) and (23).

APPENDIX B: PHYSICAL INTERPRETATION OF THE ALTERNATIVE STATE VARIABLE Θ

As discussed previously, θ is, in general, proportional to the apparent age of load-supporting contacts [Dieterich, 1979a]. Furthermore, if evolution law 1 is used, then θ equals the age of the contacts. Under conditions of constant normal stress, this definition of θ has some benefit for earthquake applications because θ is then equal to the elapsed time since the last earthquake slip, in the absence of subsequent fault creep. However, under conditions of variable normal stress, the interpretation of θ as apparent age of contacts loses its simplicity. For example, from (14), in the absence of any slip, if normal stress increases sufficiently rapidly, then the apparent age of contacts will decrease with elapsed time. Alternatively, if normal stress decreases, then the apparent age of contacts will increase more rapidly than elapsed time.

While θ has been given a physical interpretation, Θ has not. However, according to (17), θ and Θ apparently represent the same physical process. We offer a brief interpretation of Θ , consistent with classical friction theory and paralleling the argument given by Dieterich [1979a] that θ represents the apparent age of the load-bearing contacts. We make the usual assumption that frictional strength is proportional to the real area of load-bearing contacts, as in the approach of Bowden and Tabor [1964]:

$$\tau = p(V)a = [p_0 + p_1 \ln (V/V^*)]a, \quad (26)$$

where a is contact area per unit area, which, in turn, is generally proportional to normal stress. For this discussion the shear strength coefficient $p(V)$ has a slip rate dependence of the type given in (3) and in (26). If we assume that the mechanism for state-related changes in friction involves changes in contact area due to time-dependent asperity creep [Dieterich and Conrad, 1984], then

$$a = a_i + a_\Theta, \quad (27)$$

where a_i is the elastic component of contact area and a_Θ is the portion of the contact area resulting from time-dependent creep. Substituting (27) into (26) gives

$$\tau = a_i p_0 + a_i p_1 \ln (V/V^*) + a_\Theta p_0 + a_\Theta p_1 \ln (V/V^*). \quad (28)$$

Since the rate- and state-dependent variations in frictional strength are small in relation to the nominal frictional strength, the term $a_\Theta p_1 \ln (V/V^*)$ is of second order. Dropping this term in (28), the three remaining terms correspond, term by term, to those in (18) with

$$\begin{aligned} \mu^* \sigma &= a_i p_0, \\ A\sigma \ln (V/V^*) &= a_i p_1 \ln (V/V^*), \end{aligned} \quad (29)$$

$$B\sigma \Theta = a_\Theta p_0.$$

Hence Θ is interpreted to be linearly proportional to that fraction of the contact area associated with time-dependent creep.

In summary, the state-dependent variation in the resistance to sliding that occurs in response to changes in slip rate and changes in normal stress can be described by either parameter, θ or Θ . Equation (17) gives the relationship between the two variables, θ and Θ , both of which can be interpreted to represent the time-dependent growth of the load-bearing contacts. The resistance to sliding is linearly proportional to the apparent contact area whose time-dependent part is linearly proportional to Θ and logarithmically proportional to θ .

Acknowledgments. P. G. Okubo, P. Segall, T. E. Tullis, and T.-f. Wong provided careful reviews which helped greatly in clarifying our presentation. In addition, P. G. Okubo and D. A. Lockner provided valuable technical assistance in the laboratory. M.F.L. would also like to acknowledge M. D. Zoback, D. D. Pollard, and the Stanford Geophysics Department for their encouragement and support during the middle stages of this work.

REFERENCES

- Biegel, R. L., C. G. Samis, and J. H. Dieterich, The frictional properties of a simulated gouge having a fractal particle distribution, *J. Struct. Geol.*, **11**, 827-846, 1989.
- Blanpied, M. L., and T. E. Tullis, The stability and behavior of a frictional system with a two state variable constitutive law, *Pure Appl. Geophys.*, **124**, 415-444, 1986.
- Bowden, F. P., and D. Tabor, *The Friction and Lubrication of Solids*, Clarendon, Oxford, 1964.
- Byerlee, J., Friction of rocks, *Pure Appl. Geophys.*, **116**, 615-626, 1978.
- Chester, F. M., Temperature and rate dependence of friction for faults (abstract), *Eos Trans. AGU*, **69**, 471, 1988.
- Dieterich, J. H., Time-dependent friction in rocks, *J. Geophys. Res.*, **77**, 3690-3697, 1972.
- Dieterich, J. H., Time-dependent friction and the mechanics of stick-slip, *Pure Appl. Geophys.*, **116**, 790-806, 1978.
- Dieterich, J. H., Modeling of rock friction, 1, Experimental results and constitutive equations, *J. Geophys. Res.*, **84**, 2161-2168, 1979a.
- Dieterich, J. H., Modeling of rock friction, 2, Simulation of preseismic slip, *J. Geophys. Res.*, **84**, 2169-2175, 1979b.
- Dieterich, J. H., Constitutive properties of faults with simulated gouge, in *Mechanical Behavior of Crustal Rocks*, *Geophys. Monogr. Ser.*, vol. 24, edited by N. L. Carter, M. Friedman, J. M. Logan, and D. W. Stearns, pp. 103-120, AGU, Washington, D. C., 1981.
- Dieterich, J. H., A model for the nucleation of earthquake slip, in *Earthquake Source Mechanics*, *Geophys. Monogr. Ser.*, vol. 37,

- edited by S. Das, J. Boatwright, and C. H. Scholz, pp. 37–47, AGU, Washington, D. C., 1986.
- Dieterich, J. H., Nucleation and triggering of earthquake slip: Effect of periodic stresses, *Tectonophysics*, *144*, 127–139, 1987.
- Dieterich, J. H., Probability of earthquake recurrence with non-uniform stress rates and time-dependent failure, *Pure Appl. Geophys.*, *126*, 589–617, 1988.
- Dieterich, J. H., and G. Conrad, Effect of humidity on time- and velocity-dependent friction in rocks, *J. Geophys. Res.*, *89*, 4196–4202, 1984.
- Gu, J.-c., J. R. Rice, A. L. Ruina, and S. T. Tse, Slip motion and stability of a single degree of freedom elastic system with rate and state dependent friction, *J. Mech. Phys. Solids*, *32*, 167–196, 1984.
- Hobbs, B. E., and B. H. G. Brady, Normal stress changes and the constitutive law for rock friction (abstract), *Eos Trans. AGU*, *66*, 382, 1985.
- Horowitz, F. G., Mixed state variable laws; Some implications for experiments and a stability analysis (abstract), *Eos Trans. AGU*, *69*, 471–472, 1988.
- Horowitz, F. G., and A. Ruina, Slip patterns in a spatially homogeneous fault model, *J. Geophys. Res.*, *94*, 10,279–10,298, 1989.
- Koslov, D. D., and H. P. Liu, Reformulation and discussion of mechanical behavior of the time-dependent friction law proposed by Dieterich, *Geophys. Res. Lett.*, *7*, 913–916, 1980.
- Lockner, D. A., R. Summers, and J. D. Byerlee, Effects of temperature and sliding rate on frictional strength of granite, *Pure Appl. Geophys.*, *124*, 445–485, 1986.
- Marone, C., C. B. Raleigh, and C. H. Scholz, Frictional behavior and constitutive modeling of simulated fault gouge, *J. Geophys. Res.*, *95*, 7007–7025, 1990.
- Marone, C. J., C. H. Scholz, and R. Bilham, On the mechanics of earthquake afterslip, *J. Geophys. Res.*, *96*, 8441–8452, 1991.
- Mavko, G. M., S. Schulz, and B. D. Brown, Effects of the 1983 Coalinga, California earthquake on creep along the San Andreas fault, *Bull. Seismol. Soc. Am.*, *75*, 475–489, 1985.
- Okubo, P. G., Experimental and numerical study of frictional instability seismic sources, Ph.D. thesis, Mass. Inst. of Technol., Cambridge, Mass., 1986.
- Okubo, P. G., Dynamic rupture modeling with laboratory-derived constitutive relations, *J. Geophys. Res.*, *94*, 12,321–12,335, 1989.
- Okubo, P. G., and J. H. Dieterich, Effect of physical fault properties on frictional instabilities produced on simulated faults, *J. Geophys. Res.*, *89*, 5817–5827, 1984.
- Okubo, P. G., and J. H. Dieterich, State variable fault constitutive relations for dynamic slip, in *Earthquake Source Mechanics, Geophys. Monogr. Ser.*, vol. 37, edited by S. Das, J. Boatwright, and C. H. Scholz, pp. 25–35, AGU, Washington, D. C., 1986.
- Olsson, W. A., The effect of normal stress history on rock friction, in *Key Questions in Rock Mechanics: Proceedings of the 29th U.S. Symposium*, edited by P. A. Cundall, R. L. Sterling, and A. M. Starfield, pp. 111–117, A. A. Balkema, Rotterdam, Netherlands, 1988.
- Rice, J. R., Constitutive relations for fault slip and earthquake instabilities, *Pure Appl. Geophys.*, *121*, 443–475, 1983.
- Rice, J. R., and J.-c. Gu, Earthquake aftereffects and triggered seismic phenomena, *Pure Appl. Geophys.*, *121*, 187–219, 1983.
- Rice, J. R., and A. L. Ruina, Stability of steady frictional slipping, *J. Appl. Mech.*, *50*, 343–349, 1983.
- Rice, J. R., and S. T. Tse, Dynamic motion of a single degree of freedom system following a rate and state dependent friction law, *J. Geophys. Res.*, *91*, 521–530, 1986.
- Ruina, A. L., Friction laws and instabilities: A quasistatic analysis of some dry friction behaviour, Ph.D. thesis, Brown Univ., Providence, R. I., 1980.
- Ruina, A. L., Slip instability and state variable friction laws, *J. Geophys. Res.*, *88*, 10,359–10,370, 1983.
- Scholz, C. H., and J. T. Engelder, The role of asperity indentation and ploughing in rock friction, 1, Asperity creep and stick-slip, *Int. J. Rock Mech. Min. Sci. Geomech. Abstr.*, *13*, 149–154, 1976.
- Simpson, R. W., S. S. Schultz, L. D. Dietz, and R. O. Burford, The response of creeping parts of the San Andreas fault to earthquakes on nearby faults: Two examples, *Pure Appl. Geophys.*, *126*, 665–685, 1988.
- Stuart, W. D., Forecast model for great earthquakes at the Nankai trough subduction zone, *Pure Appl. Geophys.*, *126*, 619–641, 1988.
- Tse, S. T., and J. R. Rice, Crustal earthquake instability in relationship to the depth variation of frictional slip properties, *J. Geophys. Res.*, *91*, 9452–9472, 1986.
- Tullis, T. E., and J. D. Weeks, Constitutive behavior and stability of frictional sliding of granite, *Pure Appl. Geophys.*, *124*, 384–414, 1986.
- Weeks, J. D., and T. E. Tullis, Frictional sliding of dolomite: A variation in constitutive behavior, *J. Geophys. Res.*, *90*, 7821–7826, 1985.
- Wong, T.-f., Y. Gu, T. Yanagidani, and Y. Zhao, Stabilization of faulting by cumulative slip, in *Fault Mechanics and Transport Properties of Rock, The Brace Volume*, edited by B. Evans and T.-f. Wong, Academic, San Diego, Calif., 1991.
- J. H. Dieterich, U.S. Geological Survey, 345 Middlefield Road, Menlo Park, CA 94025.
- M. F. Linker, Hoffman Laboratory, Department of Earth and Planetary Sciences, Harvard University, 20 Oxford Street, Cambridge, MA 02138.

(Received September 21, 1990;
revised November 13, 1991;
accepted December 27, 1991.)